Hybrid Organic–Inorganic 1D and 2D Frameworks with ε-Keggin Polyoxomolybdates as Building Blocks

Anne Dolbecq,* Pierre Mialane, Laurent Lisnard, Jérôme Marrot, and Francis Sécheresse[a]

Dedicated to Professor Pierre Gouzerh on the occasion of his 60th birthday

Abstract: Organic–inorganic hybrid materials based on polyoxometalate building blocks with capping La^{3+} ions and bidentate oxygenated ligands have been obtained by reaction at room temperature of the $[\varepsilon\text{-}PMo_{12}O_{36}(OH)_4\{La(H_2O)_4\}]^{5+}$ polyoxocation with glutarate ($C_5H_6O_2^{2-}$) and squarate ($C_4O_4^{2-}$) organic ligands. $[\varepsilon\text{-}PMo_{12}O_{37}(OH)_3\{La(H_2O)_4(C_5H_6O_4)_{0.5}\}_4]\cdot 21\,H_2O$ (**1**) and $[\varepsilon\text{-}PMo_{12}O_{39}(OH)\{La(H_2O)_6\}_2\{La(H_2O)_5(C_4O_4)_{0.5}\}_2]\cdot 17\,H_2O$ (**2**) form unprecedented 1D chains built from alternating polyoxocations and organic ligands connected through La–O links. The structures of these materials are compared to the 2D hybrid organic–inorganic framework $[NC_4H_{12}]_2[Mo_{22}O_{52}(OH)_{18}\{La(H_2O)_4\}_2\{La(CH_3CO_2)_2\}_4]\cdot 8\,H_2O$ (**3**) isolated from the hydrothermal reaction of elemental precursors (MoO_4^{2-}, Mo, La^{3+}) in acetate buffer. Compound **3** is built from previously undescribed polyoxometalate units with twenty-two Mo^V centers capped by six La^{3+} ions, four of which are bridged by acetate ligands.

Keywords: carboxylate ligands · ε-Keggin ion · molybdenum · organic–inorganic hybrid composites · polyoxometalates

Introduction

Most of the polyoxometalates (POMs) have discrete structures of definite sizes and shapes belonging to well-known structural types, such as the Lindquist (e.g. $Mo_6O_{19}^{2-}$), Keggin (e.g. $PMo_{12}O_{40}^{3-}$), or Dawson (e.g. $P_2Mo_{18}O_{62}^{6-}$) types.[1] Linking these discrete entities to build solid-state materials is of great interest not only from a structural point of view, but also because they are potentially interesting for applications in different areas such as catalysis, electrical conductivity, and biological chemistry.[2] Synergistic effects have also been invoked.[3] Three main approaches have been developed for the linkage of POM building blocks. The first way is based on the functionalization of a POM precursor with organic ligands and the subsequent or concomitant coupling of the organic derivatives (Scheme 1a). A few materials have so far been successfully obtained, namely two examples of dimers of Lindquist type POMs;[3, 4] this illustrates the efficiency of the coupling of organoimido derivatives of POMs, catalytic POM-terminated dendrimers,[5] and polymers with covalently bound POMs.[6] The second and third approaches use the coordination chemistry of POMs with transition metal ions or even lanthanides. The coupling may be direct through the metal ion or the rare-earth center bound to terminal oxygen atoms of the POM (Scheme 1b) or can occur by the intermediate of a bidentate organic ligand (Scheme 1c). Several examples of multidimensional frameworks in which transition-metal coordination complexes serve as inorganic bridging linker have recently been published.[7] In the case of lanthanide linkers, examples are less numerous and can be separated into two categories according to the nature of the POM precursor, which is either a reduced and thus highly charged and reactive POM[8] or a vacant POM.[9] Chains with $[UMo_{12}O_{42}]^{8-}$ units linked by Th^{4+} ions,[10] $[Mo_8O_{27}]^{6-}$ anions joined by Eu^{3+} ions,[11] and, more recently, $[Al(OH)_6Mo_6O_{18}]^{3-}$ POMs with La^{3+} linkers have also been reported.[12] The third approach is far less developed.[13] In almost all the previously reported

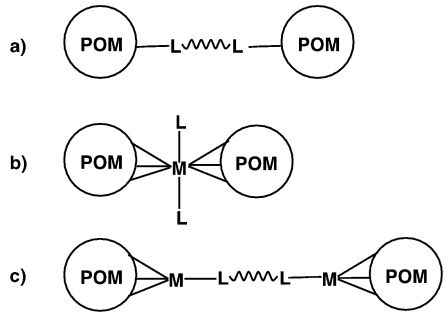

Scheme 1. Schematic representation of the three major ways to connect POM entities; M = transition metal or rare earth cation, L = organic ligand.

[a] Dr. A. Dolbecq, Dr. P. Mialane, L. Lisnard, Dr. J. Marrot, Prof. F. Sécheresse
Institut Lavoisier, IREM, UMR 8637
Université de Versailles Saint-Quentin
45 Avenue des Etats-Unis, 78035 Versailles Cedex (France)
Fax: (+33) 1-39-25-43-81
E-mail: dolbecq@chimie.uvsq.fr

DOI: 10.1002/chem.200204670

materials constructed from POM building blocks by the second and third methods described in Scheme 1, the synthesis of the materials is based on self-assembly processes and takes place either in usual bench conditions or by means of hydrothermal techniques. The rationalized synthesis of extended solids from the isolated functionalized POM precursors is still a challenge. We have recently described the synthesis of a novel polyoxocation, $[\varepsilon\text{-}PMo_{12}O_{36}(OH)_4\{La(H_2O)_4\}_4]^{5+}$ (ε-PMo_{12}), with an ε-Keggin-type core capped with four lanthanum ions.[14] The lability of the terminal water molecules on the lanthanum centers opens the way to the design of extended frameworks by reaction of the POM precursor with bidentate organic ligands. We thus describe in this paper the synthesis and structural characterization of two 1D hybrid organic–inorganic chains with ε-Keggin ions as building blocks, namely $[\varepsilon\text{-}PMo_{12}O_{37}(OH)_3\{La(H_2O)_4(C_5H_6O_4)_{0.5}\}_4]\cdot 21\,H_2O$ (**1**) with glutarate ($C_5H_6O_4^{2-}$) linkers and $[\varepsilon\text{-}PMo_{12}O_{39}(OH)\{La(H_2O)_6\}_2\{La(H_2O)_5(C_4O_4)_{0.5}\}_2]\cdot 17\,H_2O$ (**2**) with squarate ($C_4O_4^{2-}$) ligands. These materials were obtained by using the third approach described in Scheme 1. We also compare these two one-dimensional chains with the two-dimensional framework $[NC_4H_{12}]_2[Mo_{22}O_{52}(OH)_{18}\{La(H_2O)_4\}_2\{La(CH_3CO_2)_2\}_4]\cdot 8\,H_2O$ (**3**), synthesized under hydrothermal conditions, whose constituting units can be described as double ε-Keggin ions capped with lanthanum ions.

Results and Discussion

Structure of $[\varepsilon\text{-}PMo_{12}O_{37}(OH)_3\{La(H_2O)_4(C_5H_6O_4)_{0.5}\}_4]\cdot 21\,H_2O$ (1): The addition of glutarate ions to a solution of ε-PMo_{12} leads to the formation of 1D chains of polyoxocations linked by glutarate ligands (Figure 1). The compound crystallizes in the triclinic space group $P\bar{1}$, with one ε-PMo_{12} polyoxocation and two glutarate ligands in the asymmetric unit. Each lanthanum ion on the cation is linked to an organic ligand via the carboxylate moieties which act as chelating groups (Figure 2a, Table 1). Two bidentate ligands, almost parallel, thus connect the polyoxocations one by one. Four

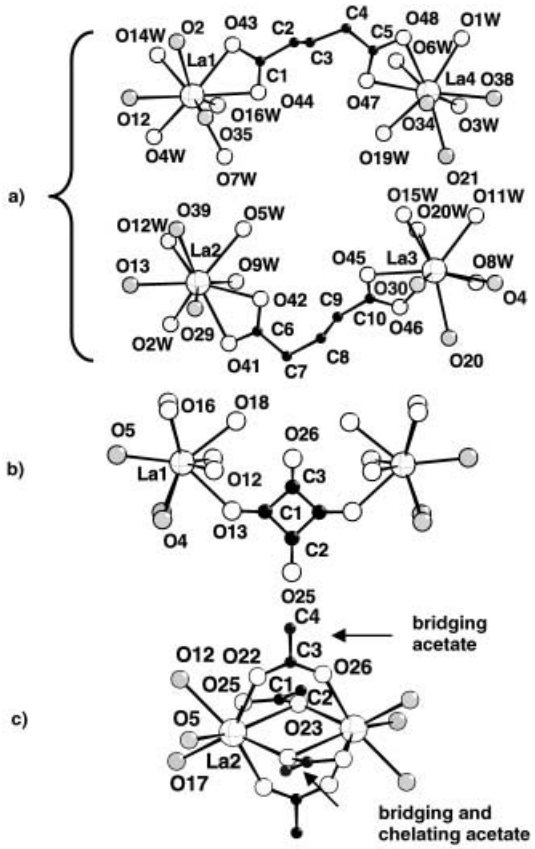

Figure 2. The different coordination geometries around the lanthanum ions in a) **1** with glutarate ligands, b) **2** with squarate ligands, and c) **3** with acetate ligands; the oxygen atoms bound to the POM core are represented by gray spheres. The corresponding bond lengths are given in Table 2.

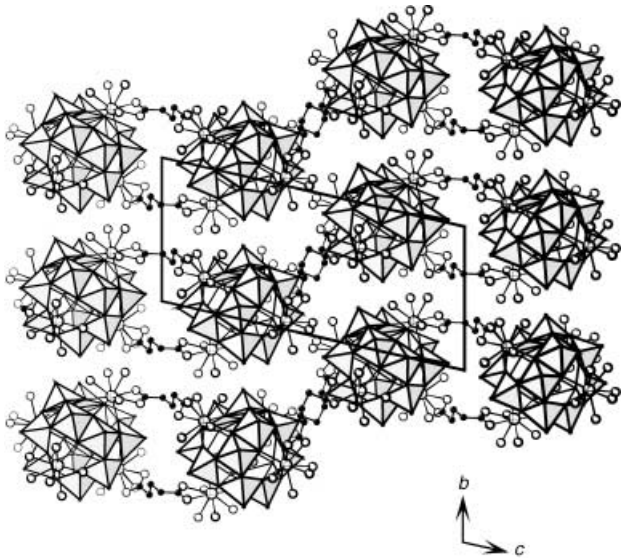

Figure 1. View of the structure of **1** along the *a* axis showing the zigzag chains of {ε-PMo_{12}} ions linked by glutarate ligands via the rare earth capping centers.

Table 1. Ranges and mean bond distances [Å] within the POM core in **1**, **2**, and **3**.

	1	**2**	**3**
P–O	1.561(8) – 1.584(8) [1.569][b]	1.543(6) – 1.553(5) [1.548]	
Mo–O_a[a]	2.425(8) – 2.679(6) [2.546]	2.472(4) – 2.633(4) [2.530]	1.857(2) – 2.334(2) [2.248]
Mo–$O_{b,c}$[a]			
Short	1.818(8) – 2.040(7) [1.954]	1.814(4) – 2.006(4) [1.927]	1.932(2) – 1.961(2) [1.952]
Long[c]	2.072(7) – 2.096(8) [2.087]	2.037(4) – 2.038(4) [2.037]	2.083(2) – 2.141(2) [2.107]
Mo–O_d[a]	1.675(9) – 1.704(7) [1.684]	1.678(6) – 1.688(6) [1.682]	1.666(3) – 1.680(2) [1.673]
Mo^V–Mo^V	2.5792(14) – 2.6069(13) [2.587]	2.566(1) [2.565]	2.5430(6) – 2.6183(13) [2.596]
Mo···Mo[d]	3.1404(14) – 3.1509(15) [3.146]	3.081(1) – 3.118(2) [3.100]	

[a] O_a refers to an oxygen atom of the central cavity, bound to the phosphorous atom in **1** and **2**, $O_{b,c}$ refers to bridging oxygen atoms, O_d refers to a terminal oxygen atom. [b] Mean values are indicated between square brackets. [c] Mo–O bond lengths for O atoms bridging two Mo atoms of the Keggin core with two corresponding Mo–$O_{b,c}$ lengths longer than 2.0 Å. [d] Mo···Mo bond lengths shorter than 3.20 Å between Mo^{VI} centers in **1** and Mo^{VI} and Mo^V centers (which are partly delocalized) in **2**.

water molecules complete the coordination sphere of the nonacoordinated lanthanum ions. As the polyoxocation does not lie on any symmetry element, the Mo–Mo bond lengths (Table 1) are not averaged, as observed in the structure of the chlorine and bromine salt of ε-PMo_{12},[14] this allows an attribution of the formal oxidation state of each metallic center to be proposed (Figure 3a). Among the twelve Mo ions, eight are Mo^{V} ions, dimerized into diamagnetic Mo^{V}–Mo^{V} pairs ($d_{Mo\text{-}Mo} = 2.60$ Å) while the remaining four are Mo^{VI} centers ($d_{Mo\text{-}Mo} = 3.10$ Å). The localization of the unpaired electrons on the Mo centers is consistent with the absence of a charge-transfer band (around 800 nm) characteristic of the "molybdenum blues" species.[15] Valence-bond calculations[16] were applied to all atoms, confirming the oxidation state of the Mo atoms (eight Mo atoms with bond valence sums (Σs) in the range 5.07–5.23 and four Mo atoms with Σs in the range 5.90–5.98); this also allows the location of the protons on the μ_2-oxygen atoms to be proposed. Four oxygen atoms bridging two Mo^{V} centers of two different Mo^{V}–Mo^{V} pairs were found to have lower valence-bond numbers ($1.21 \leq \Sigma s \leq 1.25$). In order to respect the electroneutrality of the compound, three protons were placed on the polyoxocation, therefore these three protons are supposed to be delocalized over the four bridging oxygen atoms with lower valence-bond numbers. The hybrid organic–inorganic zigzag chains stack along the *b* axis (Figure 1) forming a compact arrangement. A set of hydrogen-bonding interactions can be identified between the water molecules on the lanthanum ions, the carboxylate groups, and the terminal oxygen atoms of the adjacent chain (Figure 4).

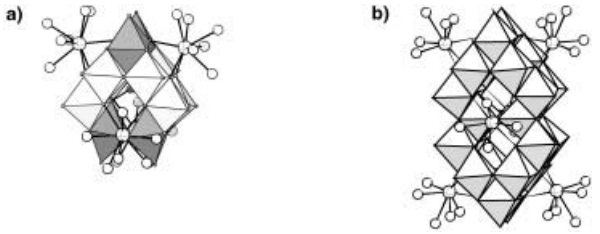

Figure 3. a) View of the structure of the molecular cation ε-PMo_{12}^{4+} in **1**, the Mo^{V} centers are represented by light gray octahedra while the Mo^{VI} centers are shown as medium gray octahedra. b) Representation of the polyoxometalate building block in **2**, showing the two interpenetrating {ε-Mo_{12}} subunits.

Table 2. Selected La–O, C–C and C–O bond distances [Å] in **1**, **2**, and **3** associated to the representations of Figure 2.

1			
La1–O35	2.486)	La3–O30	2.498(8)
La1–O44	2.571(9)	La3–O4	2.574(6)
La1–O2	2.580(7)	La3–O46	2.592(8)
La1–O4W	2.590(9)	La3–O45	2.596(8)
La1–O14W	2.5603(9)	La3–O8W	2.601(9)
La1–O12	2.609(7)	La3–O11W	2.637(9)
La1–O43	2.613(9)	La3–O20W	2.641(9)
La1–O7W	2.685(8)	La3–O15W	2.643(9)
La1–O16W	2.688(8)	La3–O20	2.661(7)
La2–O29	2.502(8)	La4–O34	2.470(7)
La2–O39	2.546(7)	La4–O1W	2.527(9)
La2–O42	2.554(7)	La4–O47	2.577(8)
La2–O2W	2.559(8)	La4–O21	2.581(7)
La2–O41	2.610(7)	La4–O38	2.590(7)
La2–O13	2.627(7)	La4–O48	2.597(7)
La2–O9W	2.632(9)	La4–O6W	2.612(8)
La2–O12W	2.640(9)	La4–O3W	2.647(8)
La2–O5W	2.701(9)	La4–O19W	2.694(10)
C1–C2	1.512(18)	C6–C7	1.506(16)
C2–C3	1.515(16)	C7–C8	1.547(16)
C3–C4	1.502(17)	C8–C9	1.509(19)
C4–C5	1.510(15)	C9–C10	1.509(16)
C5–O47	1.289(14)	C6–O41	1.273(14)
C5–O48	1.288(15)	C6–O42	1.280(14)
C1–O43	1.290(14)	C10–O45	1.270(14)
C1–O44	1.260(14)	C10–O46	1.286(14)
2			
La1–O5	2.450(6)	La1–O4	2.578(4)
La1–O12	2.566(6)	La1–O13	2.610(6)
La1–O18	2.567(8)	La1–O16	2.638(6)
C1–C3	1.40(1)	C2–O25	1.25(2)
C1–C2	1.41(1)	C3–O26	1.20(2)
3			
La2–O5	2.419(2)	La2–O22	2.506(3)
La2–O17	2.418(5)	La2–O12	2.559(2)
La2–O23	2.456(3)	La2–O25	2.575(3)
La2–O26	2.467(3)	La2–O23	2.744(3)
C1–C2	1.498(8)	C3–C4	1.461(9)
C1–O25	1.229(5)	C3–O22	1.249(5)
C1–O23	1.277(5)	C3–O26	1.228(5)

Structure of $[\varepsilon$-$PMo_{12}O_{39}(OH)\{La(H_2O)_6\}_2\{La(H_2O)_5(C_4O_4)_{0.5}\}_2] \cdot 17H_2O$ (2): The structure of the 1D chains resulting from the linkage of ε-PMo_{12} cations via the bidentate squarate ligands (Figure 5) is similar to that of **2** except that only two of the four nonacoordinated lanthanum ions are bound to an organic ligand. The squarate ligand thus bridges two La^{3+} ions through two *trans*-located μ_2-oxygen atoms, two positions remaining uncoordinated (Figure 2b, Table 1). The squarate ligand does not show significant deviations from planarity, as sometimes observed in structures of La^{III} squarates,[17] and the two La^{3+} ions lie in the plane of the organic ligand. This connecting scheme leads to the formation of a straight POM-La-squarate-La-POM chain while the infinite motif in **1** was a zigzag chain. The chains running

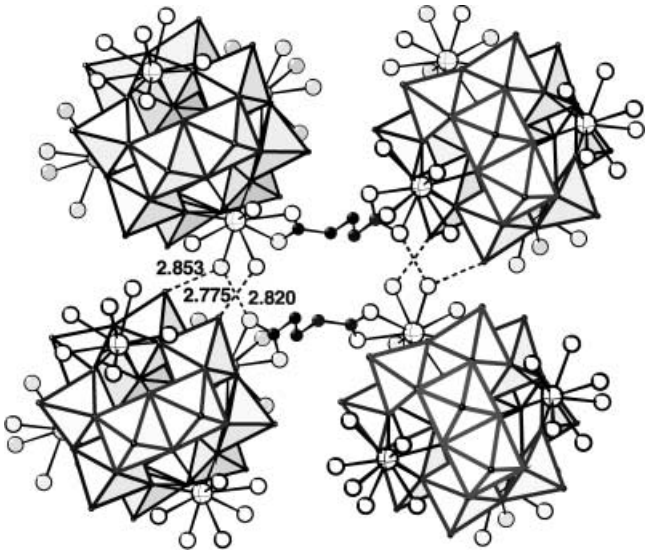

Figure 4. Hydrogen-bonding scheme, with the related O···O bond lengths, between two chains of polyoxometalates linked by glutarate ligands in **1**.

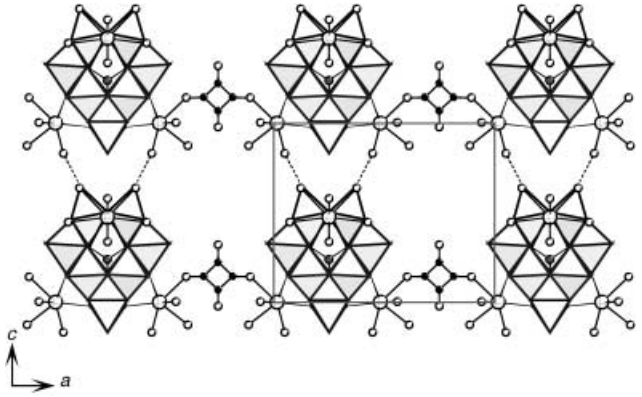

Figure 5. View along the *b* axis of the 1D chains in **2**, built from the connection of {ε-Mo_{12}} units by squarate ligands via the rare earth capping centers. Hydrogen bonds between the polyoxocations in two adjacent chains are represented as dotted lines.

parallel to the *a* axis stack on top of each other along the *c* axis forming hybrid organic–inorganic sheets. Hydrogen bonding interactions ($d_{O\cdots O} = 2.97$ Å) between two water molecules on two lanthanum ions and two terminal oxygen atoms of an {ε-PMo_{12}} core of an adjacent chain ensure the cohesion within the sheet (Figure 5). The different planes stack along the *b* axis and are shifted by *c*/2 in order to get the most compact framework.

Structure of $[NC_4H_{12}]_2[Mo_{22}O_{52}(OH)_{18}\{La(H_2O)_4\}_2\{La(CH_3CO_2)_2\}_4]\cdot 8H_2O$ (3): Compound **3** is a two-dimensional material with POM units connected in two directions by acetate ligands (Figure 6). The building block of **3** is a polyoxometalate with 22 Mo^V centers, arranged in 11 Mo^V–Mo^V pairs. A mirror plane containing a C_2 axis intersects the POM (C_{2h} symmetry). It can be viewed as the merging of two {ε-$Mo_{12}O_{40}$} POMs that have a Mo^V–Mo^V pair in common (Figure 3b). To our knowledge, this framework has never been described so far in the chemistry of POMs. As has already been observed for other POMs containing the

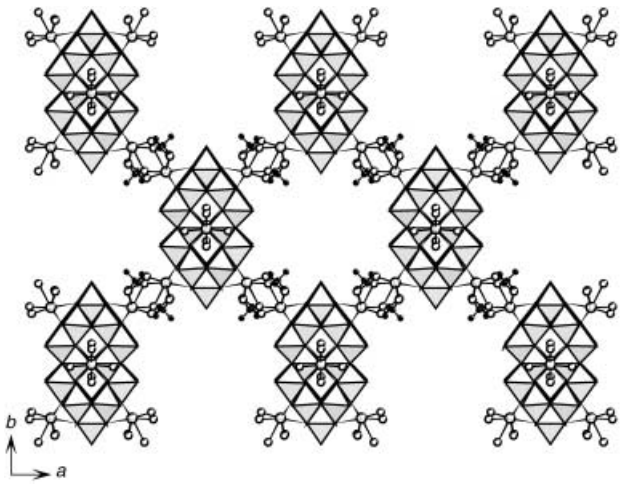

Figure 6. Representation of the 2D planes of {ε-Mo_{22}} cores linked by acetate groups via lanthanum capping centers in **3**.

{ε-$Mo_{12}O_{40}$} core,[18] the central cavity of each {ε-$Mo_{12}O_{40}$} entity is occupied by two protons. Valence-bond calculations have shown that the two protons are localized on two of the four μ_3-oxygen atoms that define the cavity perimeter. The absence of a central element within the cavity of the {ε-$Mo_{12}O_{40}$} core leads to a shortening of the Mo–O_a bond lengths (Table 1). Fourteen additional protons have been found delocalized over the sixteen μ_2-oxygen atoms. The {ε-Mo_{22}} core is stabilized by 6 La^{3+} capping ions. Four lanthanum ions are bound to the POM by three oxygen atoms and cap hexagonal $\{Mo_2\}_3$ faces in a similar manner to that observed for the parent compounds **1** and **2** containing the {ε-$PMo_{12}O_{4O}$} core (Figure 3b). The other two La^{3+} ions are located at the junction of the {ε-$Mo_{12}O_{40}$} entities. These cations are connected to the two {ε-$Mo_{12}O_{40}$} subunits via four oxygen atoms and to a μ_2-oxygen atom bridging the Mo^V–Mo^V pair common to the two interpenetrating {ε-$Mo_{12}O_{40}$} entities. Four additional water molecules are bound to these two La^{3+} ions, which are thus nonacoordinated. The four remaining rare earth centers are octacoordinated and are connected to four acetate groups that bridge two La^{3+} ions of two neighboring POMs. Two coordination geometries may be distinguished for the acetate groups (Figure 2c, Table 1): two acetates bridge in the more common $\eta^1{:}\eta^1{:}\mu_2$ fashion and the other two bridge in the rarer $\eta^2{:}\eta^1{:}\mu_2$ mode; these latter acetate groups are both bridging and chelating groups. Indeed, the two oxygen atoms are bound to the same lanthanum ion, one of the oxygen atoms being also connected to the other La^{3+} ion in a μ_2-bridging manner. Consequently the C–O bond lengths within the bridging groups (C3–O22 and C3–O26, Table 1) are equivalent, while the C1–O23 bond length is longer than the C1–O25 length in the bridging and chelating carboxylate groups. This connecting scheme of two rare earth centers with four bridging acetate groups has already been observed a few times[19] and allows the rare earth ions to be brought closer ($d_{La\cdots La} = 4.12$ Å). One POM is thus linked to four adjacent POMs, forming a 2D plane (Figure 5). The different planes are shifted by *a*/2 and stack along the *c* axis. $(C_2H_5)_2NH_2^+$ counterions are interleaved between the sheets.

^{31}P NMR spectroscopy: A ^{31}P NMR spectroscopy study was performed in order to investigate the reactivity of the ε-PMo_{12} parent polyoxocation toward organic oxygenated ligands. As the addition of glutaric or squaric acids leads to the quick precipitation of an insoluble powder, we chose the acetate ligands for which the precipitation is slower, especially at low reaction pH. The ^{31}P NMR spectrum of ε-PMo_{12} in water reveals two resonances δ_1 and δ_2, located at 1.52 and 1.06 ppm, respectively, and with relative intensities 1:5.5 (Figure 7). These two peaks have been attributed[14] to the parent ε-PMo_{12} ion (δ_2) and the derived species with three capping La^{3+} ions (δ_1) according to the following Equilibrium (1):

$$[\varepsilon\text{-}PMo_{12}O_{36}(OH)_4\{La(H_2O)_4\}_4]^{5+} \rightleftharpoons [\varepsilon\text{-}PMo_{12}O_{36}(OH)_4\{La(H_2O)_4\}_3]^{2+} + La^{3+} + 4H_2O \quad (1)$$

The addition of increasing amounts of acetic acid in an aqueous solution of ε-PMo_{12} leads to a continuous decrease of

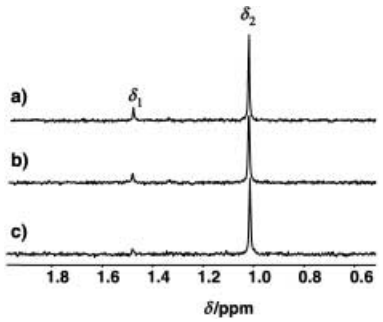

Figure 7. ^{31}P NMR spectra of an aqueous solution of $[\varepsilon\text{-}PMo_{12}O_{36}(OH)_4\{La(H_2O)_4\}_4]^{5+}$ (ε-PMo_{12}) to which had been added variable amounts of CH_3COOH; the ratios of initial concentrations were a) $[CH_3COOH]^0/[\varepsilon\text{-}PMo_{12}]^0 = 0$, b) $[CH_3COOH]^0/[\varepsilon\text{-}PMo_{12}]^0 = 4$, c) $[CH_3COOH]^0/[\varepsilon\text{-}PMo_{12}]^0 = 40$.

the δ_1 resonance until it almost disappears for $[CH_3COOH]^0/[\varepsilon\text{-}PMo_{12}]^0 = 40$. This result shows that acetic acid reacts with the POM and stabilizes the species with four La^{3+} ions relative to the species with three La^{3+} ions that is, it drives Equilibrium (1) to the left. This can be explained by the greater affinity of acetate ions for the most highly positively charged species. Although the existence of Equilibrium (1) could have been expected to lead to a mixture of species (according to the number of capping rare earth ions), the addition of an organic ligand to ε-PMo_{12} stabilizes the tetracapped polyoxocation. This result is confirmed by the synthesis of **1** and **2** as a pure phase and in good yield.

Synthesis of organic–inorganic solid-state materials: The synthesis of 1D hybrid organic–inorganic chains is quite straightforward, starting from an aqueous solution of the ε-Keggin precursor $[\varepsilon\text{-}PMo_{12}O_{36}(OH)_4\{La(H_2O)_4\}_4]^{5+}$[14] to which an excess of the organic ligand is added. A burgundy crystalline powder, insoluble in water and in the most common organic solvents, immediately precipitates. Single crystals suitable for X-ray diffraction can be obtained from slow evaporation of a solution containing the polyoxocation and a stoichiometric amount of the organic ligand. It should be noted that these two compounds seem to be thermodynamically very stable as they have been observed as the only reaction products, with a lowered reaction yield however, even for low ligand/POM ratios, although other reaction products such as dimers or trimers of POMs could have been expected. The pH of the reaction is also a determining factor since for a low pH (pH < 2.1) no reaction occurs, a higher pH increases the yield and the kinetics of the reaction. The pH should, however, not exceed 4.0 as the decomposition of the cation occurs at higher pH values. Furthermore, the lower pK_a values of squaric acid (~1 and 3.5) compared with glutaric acid (4.3 and 5.4) explain why a lower reaction pH and a lower ligand/POM ratio are needed with the squarate ligands to obtain a quantitative precipitation of the linear POM-La-squarate-La-POM chain compared with the formation of the POM-La-glutarate-La-POM chains with the glutarate ions. Finally, the absence of chlorine, proved by elemental analysis, either in **1** and **2** indicates that the chlorine atoms initially located on the lanthanum centers in the precursor are labile and are exchanged by water molecules when dissolved in water, as ^{31}P NMR experiments had previously shown.[14]

The synthesis of the two-dimensional array is quite different since it involves the reaction of the elemental precursors, sodium molybdate, hydrazine, metallic Mo, and lanthanum chloride in an acetate buffer, the pH being adjusted with diethyl amine, under hydrothermal conditions. The presence of both hydrazine and Mo as reducing agents seems necessary for the formation of **3**, since no compound was obtained if only one of these reactants was used. The compound appears to be soluble in water; this probably corresponds to the breaking of the acetato bridges, giving a pale orange solution that slowly reprecipitates. Indeed no absorption bands corresponding to the acetate vibrations are detected in the infrared spectrum of the resulting insoluble powder; this shows the decomposition of the two-dimensional framework. Attempts to synthesize an analogous material with phosphate ions in the cavity of the ε-Keggin derivative have so far failed.

Conclusion

The synthesis of 1D chains $[\varepsilon\text{-}PMo_{12}O_{37}(OH)_3\{La(H_2O)_4(C_5H_6O_4)_{0.5}\}_4]\cdot 21H_2O$ and $[\varepsilon\text{-}PMo_{12}O_{39}(OH)\{La(H_2O)_6\}_2\{La(H_2O)_5(C_4O_4)_{0.5}\}_2]\cdot 17H_2O$ validates the two-step synthetic protocol and the capacity of $\{\varepsilon\text{-}PMo_{12}\}$ to act as a precursor for the synthesis of hybrid organic–inorganic materials. This work can be extended to various organic linkers, provided they have a sufficient affinity for lanthanum ions. The dimensionality of the materials could thus be controlled by varying the rigidity, the nature and the number of functionalities on these ligands. Furthermore, the synthesis of the 2D solid $[NC_4H_{12}]_2[Mo_{22}O_{52}(OH)_{18}\{La(H_2O)_4\}_2\{La(CH_3CO_2)_2\}_4]\cdot 8H_2O$ shows that hydrothermal techniques offer a complementary way for the synthesis of multidimensional hybrid organic–inorganic materials.

Experimental Section

Synthesis of $[\varepsilon\text{-}PMo_{12}O_{37}(OH)_3\{La(H_2O)_4(C_5H_6O_4)_{0.5}\}_4]\cdot 21H_2O$ (1). $[\varepsilon\text{-}PMo_{12}O_{36}(OH)_4\{La(H_2O)_{2.5}Cl_{1.25}\}_4]\cdot 27H_2O$ (0.050 g, 1.45×10^{-5} mol) was dissolved in water (3 mL). Glutaric acid (0.040 g, 2.9×10^{-4} mol) was added and the pH was adjusted to 3.5 by addition of NaOH (0.1M). A burgundy microcrystalline powder (0.038 g, yield 89%) immediately precipitated and was collected by filtration, washed with EtOH, and dried with Et_2O. A few single crystals were obtained by slow evaporation of a solution of $[\varepsilon\text{-}PMo_{12}O_{36}(OH)_4\{La(H_2O)_{2.5}Cl_{1.25}\}_4]\cdot 27H_2O$ (10 mL, 0.033 g, 10^{-5} mol) to which a glutaric acid solution (2 mL, 10^{-2}M, 2×10^{-5} mol) was added. A comparison of the infrared spectra of the powder and the crystals and of the simulated (from the single-crystal diffraction data) and the experimental X-ray-diffraction powder pattern show that the same product is obtained either in good yield as a microcrystalline powder by addition of an excess of glutaric acid or as crystals by addition of a stoichiometric amount of ligand. IR (KBr pellets): $\tilde{\nu}$ = 1632s, 1532s, 1465m, 1443m, 1431m, 1404w, 963m, 922s, 813m, 765s, 696w, 664w, 600m, 557w, 518w, 479w, 346 cm^{-1} w; elemental analysis calcd (%) for $C_{10}H_{89}La_4Mo_{12}PO_{85}$: C 3.63, La 16.80, Mo 34.81, P 0.94; found C 3.66, La 16.17, Mo 35.23, P 1.24.

Synthesis of $[\varepsilon\text{-}PMo_{12}O_{39}(OH)\{La(H_2O)_6\}_2\{La(H_2O)_5(C_4O_4)_{0.5}\}_2]\cdot 17H_2O$ (2). Single crystals were obtained by slow evaporation of a solution of $[\varepsilon\text{-}PMo_{12}O_{36}(OH)_4\{La(H_2O)_{2.5}Cl_{1.25}\}_4]\cdot 27H_2O$ (10 mL, 0.033 g, 10^{-5} mol) to which squaric acid solution (1 mL, 10^{-2}M, 10^{-5} mol) was added. The solution was filtered before being left for crystallization to remove a slight

precipitate of **2** which formed immediately. IR (KBr pellets): $\tilde{\nu}$ = 1649s, 1500s, 1178w, 1085w, 984m, 966m, 930s, 802s, 765s, 694m, 596s, 530m, 484m, 346 cm^{-1} w; Compound **2** can be obtained quantitatively as a powder, starting from a solution of $[\varepsilon\text{-}PMo_{12}O_{36}(OH)_4\{La(H_2O)_{2.5}Cl_{1.25}\}_4]\cdot 27H_2O$ (10 mL, 0.100 g, 3 10^{-5} mol) to which a squaric acid solution (6 mL, 10^{-2} M, 6×10^{-5} mol) was added. The pH of the solution was adjusted to 3.0. The burgundy precipitate (0.069 g, yield 75%) was collected by filtration, washed with EtOH, and dried with Et_2O. The experimental diffraction powder pattern of the obtained powder was shown to be identical to the simulated powder pattern of **2**. Elemental analysis revealed the presence of squaric acid as an amorphous impurity; elemental analysis calcd (%) for $C_8H_{81}La_4Mo_{12}O_{87}P$: C 2.90, La 16.56, Mo 34.81, P 0.94; found C 3.16, La 16.40, Mo 34.73, P 1.05.

Synthesis of $[NC_4H_{12}]_2[Mo_{22}O_{52}(OH)_{18}\{La(H_2O)_4\}_2\{La(CH_3CO_2)_2\}_4]\cdot 8H_2O$ (3). A mixture of $Na_2MoO_4\cdot 2H_2O$ (0.190 g, 0.78 mmol), $N_2H_4\cdot H_2O$ (0.019 mL, 0.39 mmol), Mo (0.038 g, 0.39 mmol), $LaCl_3\cdot 7H_2O$ (0.139 g, 0.39 mmol), CH_3COOH (2 mL), and water (3 mL) (pH adjusted to 4.5 with diethyl amine) was sealed in a Teflon-lined reactor which was kept at 210 °C for 48 h. Dark red parallepipedic crystals were isolated from a gray powder by decantation and washed with EtOH (0.039 g, 15% yield in crystals, based on Mo). IR (KBr pellets): $\tilde{\nu}$ = 1589s, 1561s, 1445s, 1412m, 1345w, 1050w, 1022w, 975s, 805s, 729s, 683m, 665m, 520m, 428 cm^{-1} w; elemental analysis calcd (%) for $C_{24}H_{98}La_6Mo_{22}N_2O_{102}$: C 5.85, La 16.93, Mo 42.86, N 0.57; found C 7.39, La 18.99, Mo 42.39, N 0.88. The deviancy from calculated and experimental results for La and C elements can be explained by the presence of $La(CH_3COO)_3\cdot 2H_2O$ impurities (ca. 9%).

NMR measurements: ^{31}P NMR spectra were recorded on a Bruker AC-300 spectrometer operating at 121.5 MHz in 5 mm tubes. ^{31}P NMR chemical shifts are referenced to the usual external standard: 85% H_3PO_4. The initial concentration of ε-PMo_{12} was $[\varepsilon\text{-}PMo_{12}]^0 = 16.67\times10^{-3}$ M. Increasing amounts of a solution of acetic acid (1M) were added in the NMR tube. The pH of the solution (2.2) remained constant during the addition of acetic acid.

X-ray crystallography. Intensity data collection was carried out with a Siemens SMART three-circle diffractometer equipped with a CCD detector with $Mo_{K\alpha}$ monochromatized radiation (λ = 0.71073 Å). The absorption correction was based on multiple and symmetry-equivalent reflections in the data set by using the SADABS program[19] based on Blessing's method.[20] The structure was solved by direct methods and refined by full-matrix least-squares by using the SHELX-TL package.[21] In the structure of **3**, the lanthanum atom not bound to the squarate ligand and its coordination sphere of water molecules is disordered over two positions. These disordered atoms were refined isotropically, the other atoms being refined anisotropically. Crystallographic data are given in Table 3. Selected bond distances are listed in Tables 1 and 2. CCDC-199669–199671 contain the supplementary crystallographic data for the structures of **1**–**3**, respectively. These data can be obtained free of charge via www.ccdc.cam.ac.uk/conts/retrieving.html (or from the Cambridge Crystallographic Data Center, 12 Union Road, Cambridge, CB2 1EZ, UK; fax:(+44) 1223-336033; or deposit@ccdc.cam.ac.uk).

Acknowledgement

A.D. and P.M. thank Prof. G. Hervé for fruitful discussions.

[1] M. T. Pope, *Heteropoly and Isopoly Oxometalates*, Springer, Berlin, **1983**.

[2] D. E. Katsoulis, *Chem. Rev.* **1998**, *98*, 359.

[3] M. Lu, Y. Wei, B. Xu, C. F.-X. Cheung, Z. Peng, D. R. Powell, *Angew. Chem.* **2002**, *114*, 1636; *Angew. Chem. Int. Ed*. **2002**, *41*, 1566.

[4] J. L. Stark, A. L. Rheingold, E. Maatta, *J. Chem. Soc. Chem. Commun.* **1995**, 1165.

[5] H. Zeng, G. R. Newkome, C. L. Hill, *Angew. Chem.* **2000**, *112*, 1841; *Angew. Chem. Int. Ed*. **2000**, *39*, 1771.

[6] a) P. Judenstein, *Chem. Mater*. **1992**, *4*, 4; b) C. R. Mayer, R. Thouvenot, T. Lalot, *Chem. Mater*. **2000**, *12*, 257; c) R. C. Schroden, C. F. Blanford, B. J. Melde, B. J. S. Johnson, A. Stein, *Chem. Mater*. **2001**, *3*, 1074; d) C. Sanchez, G. J. de A. A. Soller-Illia, F. Ribot, T. Lalot, C. R. Mayer, V. Cabuil, *Chem. Mater*. **2001**, *13*, 3061 and references therein.

[7] a) C.-M. Liu, D.-Q. Zhang, M. Xiong, D.-B. Zhu, *Chem. Commun*. **2002**, 1416; b) J.-Y. Niu, Q. Wu, J-P. Wang, *J. Chem. Soc*. *Dalton Trans.* **2002**, 2512; c) W.-M. Bu, L. Ye, G.-Y. Yang, J.-S. Gao, Y.-G. Fan, M.-C. Shao, J.-Q. Xu, *Inorg. Chem. Commun*. **2001**, *4*, 1; d) M. I. Khan, *J. Solid State Chem*. **2000**, *152*, 105 and references therein; e) D. J. Chesnut, D. Hagrman, P. J. Zapf, R. P. Hammond, R. Laduca, R. C. Haushalter, J. Zubieta, *Coord. Chem. Rev*. **1999**, *192*, 737; f) A. Müller, M. Koop , P. Schiffels, H. Bögge, *J. Chem. Soc. Chem. Commun.* **1997**, 1715; g) J. R. D. Debord, R. C. Haushalter, L. M. Meyer, D. J. Rose, P. J. Zapf, J. Zubieta, *Inorg. Chim. Acta* **1997**, *256*, 165; h) I. Loose, M. Bösing, R. Klein, B. Krebs, R. P. Schultz, B. Scharbert, *Inorg. Chim. Acta* **1997**, *263*, 99; i) J. Galan-Mascaros, C. Gimenez-Saiz, S. Tricki,

Table 3. X-ray crystallographic data for **1**, **2**, and **3**.

	1	**2**	**3**
formula	$C_{10}H_{89}La_4Mo_{12}O_{85}P$	$C_4H_{79}La_4Mo_{12}O_{83}P$	$C_{24}H_{98}La_6Mo_{22}N_2O_{102}$
M_w [g]	3306.9	3300.0	4991.2
crystal system	triclinic	orthorhombic	orthorhombic
space group	$P\bar{1}$	Pmmn	*Cmca*
Z	2	2	4
T [K]	293	293	293
a [Å]	12.1754(2)	15.6072(5)	22.3280(4)
b [Å]	12.4146(2)	17.4589(5)	26.4688(4)
c [Å]	26.9169(2)	12.6083(4)	24.7324(1)
α [°]	102.722(1)	90	90
β [°]	97.946(1)	90	90
γ [°]	90.644(1)	90	90
V [Å^3]	3926.91(7)	3435.6(2)	14616.7(3)
ρ_{calc} [g cm^{-3}]	2.686	2.930	2.279
μ [mm^{-1}]	4.115	4.686	3.625
reflections collected	18612	15378	49584
unique reflections (R_{int})	11607(0.0447)	2671(0.0732)	10108(0.0680)
refined parameters	987	265	372
$R(F_o)$[a]	0.0484	0.0903	0.0548
$R_w(F_o^2)$[b]	0.1093	0.2043	0.1321

[a] $R_1 = \frac{\sum |F_o| - |F_c|}{\sum |F_c|}$. [b] $wR_2 = \sqrt{\frac{\sum w(F_o^2 - F_c^2)^2}{\sum w(F_o^2)^2}}$ with $1/w = \sigma^2F_o^2 + aP^2 + bP$ and $P = \frac{F_o^2 + 2F_c^2}{3}$; a = 0.0548, b = 0 for **1**, a = 0.0686, b = 214.57 for **2**, a = 0.0601, b = 188.23 for **3**.

C. J. Gomez-Garcia, E. Coronado, L. Ouahab, *Angew. Chem*. **1995**, *107*, 1601; *Angew. Chem*. *Int. Ed. Engl.* **1995**, *34*, 1460; j) C. Gimenez-Saiz, J. R. Galan-Mascaros, S. Tricki, E. Coronado, L. Ouahab, *Inorg. Chem*. **1995**, *34*, 524.

[8] Although these examples do not belong exactly to the discussed category, as being built of giant cluster molecules, we can cite a) L. Cronin, C. Beugholt, E. Krickemeyer, M. Schmidtmann, H. Bögge, P. Kögerler, T. K. K. Luong, A. Müller, *Angew. Chem*. **2002**, *114*, 2929; *Angew. Chem*. *Int. Ed.* **2002**, *41*, 2805; b) G. Liu, Y.-G. Wei, Q. Yu, Q. Liu, S.-W. Zhang, *Inorg. Chem. Commun*. **1999**, *2*, 434.

[9] a) M. Sadakane, M. H. Dickman, M. T. Pope, *Angew. Chem*. **2000**, *112*, *3036*; *Angew. Chem*. *Int. Ed.* **2000**, *39*, 2914; b) P. Mialane, L. Lisnard, A. Mallard, J. Marrot, E. Antic-Fidancev, P. Aschehoug, D. Vivien, F. Sécheresse, *Inorg. Chem*. **2003**, *42*, 2102.

[10] V. N. Molchanov, I. V. Tatjanina, E. A. Torchenkova, *J. Chem. Soc. Chem. Commun.* **1981**, 93.

[11] T. Yamase, H. Naruke, *J. Chem. Soc. Dalton Trans.* **1991**, 285.

[12] V. Shivaiah, P. V. N. Reddy, L. Cronin, S. K. Das, *J. Chem. Soc. Dalton Trans.* **2002**, 3781.

[13] See for example among the impressive work of J. Zubieta a) R. N. Devi, J. Zubieta, *Inorg. Chim. Acta* **2002**, *332*, 72; b) D. Hagrman, P. J. Hagrman, J. Zubieta, *Angew. Chem*. **1999**, 111, 3359; *Angew. Chem. Int. Ed.* **1999**, *38*, 3165; c) D. Hagrman, C. Zubieta, D. J. Rose, J. Zubieta, R. C. Haushalter, *Angew. Chem*. **1997**, 109, 904; *Angew. Chem. Int. Ed. Engl.* **1997**, *36*, 873.

[14] P. Mialane, A. Dolbecq, L. Lisnard, A. Mallard, J. Marrot, F. Sécheresse, *Angew. Chem*. **2002**, *114*, 2504; *Angew. Chem*. *Int. Ed.* **2002**, *41*, 2398.

[15] A. Müller, C. Serain, *Acc. Chem. Res.* **2000**, *33*, 2.

[16] N. E. Brese, M. O'Keeffe, *Acta Crystallogr.* **1991**, *B47*, 192.

[17] J. F. Petit, A. Gleizes, J. C. Trombe, *Inorg. Chim. Acta* **1990**, *167*, 51.

[18] a) M. I. Khan, Q. Chen, J. Salta, C. J. O'Connor, J. Zubieta, *Inorg. Chem*. **1996**, *35*, 1880; b) A. Müller, C. Beugholt, P. Kögerler, H. Bögge, S. Bud'ko, M. Luban, *Inorg. Chem*. **2000**, *39*, 5176.

[19] a) S. Niu, Z. Yang, Q. Yang, B. Yang, J. Chao, G. Yang, E. Z. Shen, *Polyhedron* **1997**, *16*, 1629; b) A. Panagiotopoulos, T. F. Zafiropoulos, S. P. Perlepes, E. Bakalbassis, I. Masson-Ramade, O. Kahn, A. Terzis, C. P. Raptopoulou, *Inorg. Chem*. **1995**, *34*, 4918; c) A. Ouchi, Y. Suzuki, Y. Ohki, Y. Koizumi, *Coord. Chem. Rev*. **1988**, *92*, 29.

Received: December 16, 2002 [F4670]